A short-term model of COPD identifies a role for mast cell tryptase

Emma L. Beckett, B Biomed Sci,[a1] Richard L. Stevens, PhD,[b,c1] Andrew G. Jarnicki, PhD,[a1] Richard Y. Kim, B Biomed Sci,[a] Irwan Hanish, BSc,[a] Nicole G. Hansbro, PhD,[a] Andrew Deane, BSc,[a] Simon Keely, PhD,[a] Jay C. Horvat, PhD,[a] Ming Yang, MD, PhD,[a] Brian G. Oliver, PhD,[d] Nico van Rooijen, PhD,[e] Mark D. Inman, MD, PhD,[f] Roberto Adachi, MD,[g] Roy J. Soberman, MD,[b,h] Sahar Hamadi,[c] Peter A. Wark, MD, PhD,[a,i] Paul S. Foster, PhD,[a] and Philip M. Hansbro, PhD[a]

Newcastle, Australia, Boston, Mass, Sydney, Australia, Amsterdam, The Netherlands, Hamilton, Canada, Houston, Texas

From the [a]Priority Research Centre for Asthma and Respiratory Disease and Hunter Medical Research Institute, The University of Newcastle, Newcastle; [b]Department of Medicine, Harvard Medical School and [c]Brigham and Women's Hospital, Boston; [d]Sydney Medical School and Woolcock Institute of Medical Research, University of Sydney, Sydney; [e]Department of Molecular Cell Biology, Vrije Universiteit Medical Center, Amsterdam; [f]Firestone Institute for Respiratory Health, St Joseph's Healthcare, Hamilton; [g]Department of Pulmonary Medicine, The University of Texas MD Anderson Cancer Center, Houston; [h]Massachusetts General Hospital, Boston; and [i]Department of Respiratory and Sleep Medicine, John Hunter Hospital, Newcastle.

[1]Authors contributed equally.

Corresponding author: Professor Philip Hansbro, PhD, Priority Research Centre for Asthma and Respiratory Disease and Hunter Medical Research Institute, The University of Newcastle, Newcastle, NSW 2308, Australia. E-mail: Philip.Hansbro@newcastle.edu.au

Supported by grants from the National Health and Medical Research Council of Australia (510762, 569219, 1003565, 1003593, 1023131), the National Institutes of Health USA (AI065858 and AI059746), and the Harvard Club of Australia Foundation. We thank Dr. Julia Charles (Brigham and Women's Hospital, Boston, Mass) for her assistance in the generation of mouse bone marrow-derived macrophages.

Disclosure of potential conflict of interest: The authors declare that they have no relevant conflicts of interests.

Abbreviations used

BALF: bronchoalveolar lavage fluid

B6: C57BL/6

Cdyn: dynamic compliance

CFU: colony forming unit

COPD: chronic obstructive pulmonary disease

FEV_{100}: forced expiratory volume in 100 milliseconds

FRC: functional residual capacity

FVC: functional vital capacity

IFN-γ: interferon-γ

MC: mast cell

mMCP: mouse MC protease

MSC: mucus-secreting goblet cell

qPCR: quantitative polymerase chain reaction

PFU: plaque forming unit

PV: pressure/volume

RI: resistance

TLC: total lung capacity

TNF-α: tumor necrosis factor-α

WT: wild-type

ABSTRACT

Background: Cigarette smoke-induced chronic obstructive pulmonary disease (COPD) is a life-threatening inflammatory disorder of the lung. The development of effective therapies for COPD has been hampered by the lack of an animal model that mimics the human disease in a short time-frame.

Objectives: To create an early onset mouse model of cigarette smoke-induced COPD that develops the hallmark features of the human condition in a short time-frame. To use this model to better understand pathogenesis and the roles of macrophages and mast cells (MCs) in COPD.

Methods: Tightly controlled amounts of cigarette smoke were delivered to the airways of mice, and the development of the pathological features of COPD was assessed. The roles of macrophages and MC tryptase in pathogenesis were evaluated using depletion and *in vitro* studies and MC protease-6 deficient mice.

Results: After just 8 weeks of smoke exposure, wild-type mice developed chronic inflammation, mucus hypersecretion, airway remodeling, emphysema, and reduced lung function. These characteristic features of COPD were glucocorticoid-resistant and did not spontaneously resolve. Systemic effects on skeletal muscle and the heart, and increased susceptibility to respiratory infections also were observed. Macrophages and tryptase-expressing MCs were required for the development of COPD. Recombinant MC tryptase induced pro-inflammatory responses from cultured macrophages.

Conclusion: A short-term mouse model of cigarette smoke-induced COPD was developed in which the characteristic features of the disease were induced more rapidly than existing models. The model can be used to better understand COPD pathogenesis, and we show a requirement for macrophages and tryptase-expressing MCs.

Clinical implications: We describe a short-term mouse model with the hallmark features of cigarette smoke-induced COPD. We then show that the model can be used to further our understanding of the pathogenesis of COPD. We demonstrate for the first time that a MC-restricted tetramer-forming tryptase has a prominent adverse role in experimental COPD.

Capsule summary: We describe a mouse model of COPD that develops the hallmark features of the disease in just 8 weeks. Using this experimental model, we discovered detrimental roles for MC tryptase in COPD.

Key words: *cigarette smoke, COPD, inflammation, emphysema, airway remodeling, lung function, macrophage, mast cell, protease, mMCP-6, hTryptase-β*

INTRODUCTION

Cigarette smoke-induced chronic obstructive pulmonary disease (COPD) is a debilitating disorder of the lung. It is the 4th leading cause of chronic morbidity and death worldwide, and its prevalence is increasing.[1] The disease is characterized by chronic airway inflammation, mucus hypersecretion, airway remodeling, and emphysema that lead to reduced lung function and breathlessness.[2,3] Systemic effects also are observed in the skeletal muscle, heart, and other organs. Moreover, COPD patients are more susceptible to respiratory infections. Because the mechanisms that lead to COPD and its sequelae are poorly understood at the molecular level, there are no effective treatments.

A major factor that has hampered the study of COPD is the lack of a small animal model that recapitulates the hallmark features of the disease in a reasonable time frame. While lipopolysaccharide and elastase have been used to induce lung damage in rodents that somewhat resemble COPD in humans, such single-factor approaches are not representative of the complex pathology that occurs in those patients who smoke for many years.[3] Current models of smoke-induced COPD involve whole body or nose-only exposure of mice to cigarette smoke.[3] Acute models of 4 days to 4 weeks duration have been valuable for evaluating the early smoke-induced inflammatory responses in the lung. However, the smoke-exposed mice in these models do not develop emphysema or have diminished lung function.[4-8] Chronic models of >6 months duration result in airway remodeling and emphysema, but only induce mild alterations in lung function,[4,9-12] and the prolonged time needed to induce these features greatly restricts the use of these models for extensive therapeutic and mechanistic research. This is especially relevant considering the short life-span of the mouse and the substantial animal and labor expenses needed for 6-month experiments. Thus, there is a need for a mouse model of cigarette smoke-induced COPD that has all of the major features of the human condition that are induced in a shorter time frame.

Although mast cells (MCs) have been casually linked to the pathogenesis of COPD, the relevant factors exocytosed from these immune cells have not been identified.[13] MC numbers are increased in inflammatory infiltrates in COPD patients, which is associated with reduced lung function, airway remodeling and emphysema.[14,15] The levels of MC-derived human (h)Tryptase-β in sputum correlated with the severity of COPD in one study,[16] and the exposure of IL-3-dependent MCs to cigarette smoke-treated culture medium resulted in increased expression of mouse MC protease-6 (mMCP-6).[17] mMCP-6 is also known to promote inflammation, chemokine expression and macrophage and neutrophil chemotaxis,[18] which are all hallmark features of COPD. Nevertheless, the roles of hTryptase-β and mMCP-6 in COPD pathogenesis have not been investigated in depth.

Here we report the development of a mouse model of COPD in which we deliver tightly controlled amounts of cigarette smoke directly into the airways. The exposed mice exhibit the major characteristic features of COPD observed in humans after only 8 weeks of smoke exposure, thereby facilitating the discovery and/or testing of the efficacy of new therapeutics. The model also enables us to elucidate the cellular, biochemical and molecular mechanisms that underpin the pathogenesis of COPD. In that regard, we now show for the first time detrimental roles for a MC-restricted tetramer-forming tryptase in experimental COPD.

METHODS

Additional details are described in the Journal's Online Repository at **www.jacionline.org**.

Smoke exposure

Wild-type (WT) BALB/c, WT C57BL/6 (B6), and mMCP-6$^{-/-}$ B6 mice[18] were used in the study. In each experiment, 12 mice were simultaneously exposed to cigarette smoke [twelve 3R4F reference cigarettes (University of Kentucky, Lexington, Ky) twice/day, 5 times/week, for 1-12 weeks] using a custom-designed and purpose-built nose-only, directed flow inhalation and smoke-

exposure system (CH Technologies, Nj) housed in a fume and laminar flow hood (Fig S1). Each exposure lasted 75 minutes. All experiments were approved by our institutional animal ethics committee.

Airway and lung inflammation, airway remodeling, and emphysema

Airway inflammation was assessed by differential enumeration of inflammatory cells in bronchoalveolar lavage fluid (BALF).[19-22] Parenchymal inflammation was assessed by counting the inflammatory cells in 10 randomized fields (x100 magnification) of whole lung sections.[23] RNA was extracted and transcript levels were assessed by standard real-time quantitative (q)PCR assays,[24] using the primers described in Table S1.

The numbers of macrophages and MCs in lung homogenates were assessed by flow cytometry and histochemistry.[25-27] Airway remodeling was determined by measuring the number of mucus-expressing goblet cells around the airways and by assessing airway epithelium thickening.[22,23,28-30] Emphysema was assessed using the mean linear intercept technique, which is a standard method of assessing alveolar diameter and emphysema in mice.[28]

Lung function

Forced oscillation and forced maneuver techniques were used to assess lung function parameters.[25,31]

Glucocorticoid treatment

Dexamethasone (1 mg/kg in 50 µL sterile water, Sigma, St Louis, MO) was administered intranasally 3 times/week.[32] Controls were sham-treated with sterile water.

Respiratory infections

Mice were infected with mouse-adapted strains of *Streptococcus pneumoniae* intratracheally or influenza virus intranasally. Pathogen load was determined by culture or plaque assays of lung homogenates, respectively.[33-36]

Macrophage and neutrophil depletion

Lung macrophages and neutrophils were depleted by intranasal administration of liposome-encapsulated clodronate or intraperitoneal injection of anti-Ly6G antibody (1A8, Bioxcell, Lebannon, Nh), respectively, 3 times/week.[25,37]

Transcript expression in tryptase-treated macrophages

B6 mouse bone marrow-derived macrophages were cultured in the absence or presence of recombinant hTryptase-β (0.8 μg/ml, 25 nM, Promega, Madison, Wi). RNA was isolated, and qPCR assays were used to evaluate the levels of tumor necrosis factor-α (TNF-α), Cxcl1/KC, and interleukin (IL)-1β transcripts.

Statistical analyses

Data are presented as mean±SEM (n=6-8). Comparisons between two groups were made using a two-tailed Mann-Whitney Test. Multiple comparisons were made by one-way ANOVA with Tukey's post-test, or Kruskal-Wallis with Dunn's post-test, where non-parametric analyses were appropriate. Weights were assessed using one-way ANOVA (repeated measures). Analyses used GraphPad Prism Software (San Diego, CA).

RESULTS

Nose-only exposure of WT BALB/c mice to cigarette smoke induces the hallmark features of COPD

We delivered tightly controlled amounts of cigarette smoke into the nares of WT BALB/c mice for 1-12 weeks and assessed the hallmark features of COPD. Weight loss was evident within the 1st week of exposure (Fig 1, *A*). Animals lost 10% of their initial weight after 3 weeks, and only re-gained 5% of this initial weight over the remaining exposure period. In contrast, age-matched non-exposed mice steadily gained weight. Four days of exposure to cigarette smoke led to acute inflammation in the airways, characterized by increased numbers of macrophages and neutrophils in the BALF (Fig 1, *B*). Inflammation persisted and increased with the additional involvement of lymphocytes (particularly $CD8^+$ T cells) after 8-weeks. Smoke exposure also induced progressive increases in chronic parenchymal inflammation (Fig 1, *C*). This was accompanied by increased expression in the lung of the transcripts that encode TNF-α (Fig 1, *D*), Cxcl1 (Fig 1, *E*), and IL-1β (Fig 1, *F*), but not IL-6, IL-10, IL-13, or interferon-γ (IFN-γ) (data not shown). There were signs of airway remodeling with increased numbers of MSCs in the airways from week 6 and thickening of the airway epithelium from week 8 (Fig 1, *G* and *H*). Airway remodeling was accompanied by alveolar enlargement (increases in alveolar diameter, representative of emphysematous tissue destruction) after 8 weeks, which increased in severity by week 12 (Fig 1, *I*). Although there likely was a steady continuum of pathologic changes taking place in the smoke-exposed lungs of the WT mice, the results revealed the induction and progression of the disease over weeks 4-6 and 8-12, respectively.

Smoke exposure of the airways of mice resulted in reduced lung function similar to that observed in humans with COPD

Since 8 weeks of exposure was required to induce key features of COPD, other parameters were assessed at this time-point. We next investigated the effects of smoke exposure on parameters of lung function. Exposure decreased hysteresis, transpulmonary and airway-specific resistance (RI), tissue damping, and forced expiratory volume in 100 milliseconds/functional vital capacity ratio

(FEV_{100}/FVC, representative of FEV_1/FVC ratio in humans), but increased dynamic compliance (Cdyn), work of breathing, functional residual capacity (FRC), and total lung capacity (TLC) (Fig 2, *A-I*). These adverse changes in lung function likely resulted from the combination of chronic inflammation, airway remodeling, and emphysematous lesions with associated reductions in alveolar tissue and supporting airway attachments.

COPD features in the experimental model are glucocorticoid-resistant

While glucocorticoids are used to treat patients with COPD to reduce acute inflammation and the frequency of acute exacerbations,[38,39] they have limited efficacy.[40-42] Glucocorticoid treatment (either throughout, or for the last 6 weeks of 12 weeks of smoke exposure) did not prevent chronic inflammation or emphysema, nor did they suppress declines in lung function (Fig 3, *A-F*).

Smoke exposure of the airways has systemic effects

The lung is not the only organ adversely affected in humans with COPD, and systemic inflammation, loss in skeletal muscle mass, and cardiovascular disease often occur in this disease.[43] In our model, 8 weeks of exposure also induced systemic changes with significant alterations in the proportion of leukocytes in the blood. The percentage of monocytes decreased but the percentage of neutrophils and lymphocytes increased (Fig 4, *A*). Furthermore, skeletal muscle mass (i.e., the quadriceps) was reduced (Fig 4, *B*). Moreover, the hearts of smoke-exposed mice also were enlarged by ~25% and had more surrounding fatty tissue (Fig 4, *C*).

Induction of experimental COPD exacerbates respiratory infections

Chronic microbial colonization of the airways and infection-induced exacerbations are common in COPD patients.[44] When we infected mice previously exposed to smoke for 8 weeks with *S. pneumoniae* or influenza virus (and smoke exposure discontinued), pathogen burden increased

~10- and ~2.5-fold, respectively (Fig 4, *D* and *E*).

Experimental COPD does not rapidly resolve following smoking cessation

Once patients develop COPD, their clinical conditions generally do not improve significantly after smoking cessation, and often lung function further deteriorates.[2] In our model, smoke exposure for 8 weeks followed by cessation for 4 weeks did not improve airway inflammation, emphysema, lung function, or circulating leukocyte abnormalities (Fig 5, *A*-*F*). In regard to airway inflammation (Fig 5, *A*), the numbers of macrophages continued to increase, suggesting the presence of a macrophage-rich pro-inflammatory environment in the lung that underpins the progression of disease.

Experimental COPD is macrophage dependent

Numerous studies have indicated that pulmonary macrophages have prominent pathologic roles in humans with COPD.[7,9,45,46] Since increased numbers of macrophages were found in the lungs of our smoked-exposed WT mice (Fig 1, *B*), we assessed the importance of these phagocytes in the development of experimental COPD by reducing their numbers during smoke exposure using the clodronate-depletion method. Liposome-encapsulated clodronate were administered into the airways 3 times/week throughout 8 weeks of smoke exposure. Control animals were sham-treated with empty liposomes. The numbers of macrophages were then quantified in the BALF by morphology and in dispersed whole lung by flow cytometry ($F4/80^{+}$). Macrophages were depleted by 61±4% and 73±5% in smoke-exposed mice and by 25±3% and 36±2% in non-exposed controls in BALF and lung tissue, respectively. In contrast, the percentage of monocytes in the peripheral blood was unaffected. Macrophage depletion in the lung resulted in reduced smoke-induced epithelial thickening and emphysema, and protection against alterations in lung function (Fig 6, *A*-*E*). In contrast, depletion of neutrophils using the anti-Ly6G antibody approach did not suppress the effects

of smoke exposure (Fig S2). The accumulated data suggest a central role for pulmonary macrophages in our animal model of cigarette smoke-induced COPD, thereby supporting the clinical data of others that have implicated these cells in the pathogenesis of COPD in humans.[7]

Exposure of WT B6 mice to cigarette smoke also induces COPD

WT BALB/c and B6 mice respond differently in numerous disease models. To assess the general applicability of our model to another commonly used mouse strain, we examined the effects of smoke exposure on the lungs of WT B6 mice. Exposure for 8 weeks resulted in a similar profile and magnitude of weight loss, parenchymal inflammation, airway remodeling, emphysematous destruction (alveolar enlargement), and altered lung function in B6 mice compared to BALB/c mice (Fig S3, *A*-*N*).

The tetramer-forming tryptase mMCP-6 contributes to macrophage accumulation and inflammation in the airways, and is required for experimental COPD

Macrophage accumulation in the lungs of smoke-exposed mice could be caused by unknown factors released from activated MCs. Although MCs also have been implicated in the pathogenesis of COPD, the link between these two cell types and smoke-induced COPD has not been demonstrated, and the relevant MC-derived factors have not been identified.[13] Following 8 weeks of smoke exposure, the numbers of macrophages and MCs in the lung of WT B6 mice (i.e., the largest lobe in the multi-lobed right lung by flow cytometry or in the single-lobed left lung by histochemistry) increased ~3 fold in both instances (Fig 7, *A*-*C* and Fig S4).

To provide further evidence for the importance of macrophages and MCs in pathogenesis we also assessed their levels in the smoking cessation and clodronate depletion studies. In the cessation studies, the numbers of both of these cells types were elevated concomitant with the maintenance of disease (Fig 7, *A*-*C*). In the depletion studies, the suppression of macrophages but not MCs in the

lung correlated with the prevention of COPD (Fig 7, *A*-*C*). These studies provide further evidence for the pivotal role of macrophages in the pathogenesis of experimental COPD.

mMCP-6 and hTryptase-β have prominent roles in innate immunity and inflammation.[18,47] Thus, we hypothesized that mMCP-6 might play a critical role in experimental COPD, as occurs in experimental arthritis and colitis. We therefore subjected WT and mMCP-6 null ($^{-/-}$) B6 mice[18] to smoke exposure. We could not detect mMCP-6 mRNA by qPCR in the lungs of non-treated and smoke-treated WT mice, and the levels of mMCP-6 protein were below the limits of detection by SDS-PAGE immunoblot analysis. The numbers of MCs in the lungs of smoke-exposed mMCP-6$^{-/-}$ mice were not affected and were similar to those in the lungs of smoke-exposed WT mice. However, smoke-exposed mMCP-6-null mice had significantly fewer macrophages (Fig 8, *A* and *B*). The reduction in macrophage accumulation in the airways of the tryptase-deficient mice correlated with reductions in neutrophil numbers in the BALF, inflammation of the parenchyma, pro-inflammatory cytokine (e.g., TNF-α and IL-1β) and chemokine (e.g., Cxcl1) mRNA levels, and emphysematous lesions (Fig 8, *C*-*H*). While airway remodeling also was abrogated, there were no obvious differences in the lung function parameters measured between smoke-treated WT and mMCP-6$^{-/-}$ mice (Fig 8, *I* and *J*). While our accumulated data revealed adverse roles for mMCP-6 in the COPD model, other factors that remain to be identified must contribute to the deterioration in lung function in the smoke-exposed mice.

hTryptase-β induces macrophages to increase their expression of pro-inflammatory cytokines and chemokines

To confirm the link between MC tryptases and the pro-inflammatory activity of activated macrophages, we next treated cultured mouse bone marrow-derived macrophages with recombinant hTryptase-β. The tryptase induced these macrophages to markedly increase the levels of the transcripts that encode TNF-α, Cxcl1, and IL-1β (Fig 8, *K*-*M*). These changes did not occur if the

tryptase was boiled for 5 minutes before treatment. Although the mechanism by which MC tetramer-forming tryptases induce macrophages to increase the expression of these cytokines and chemokines remains to be determined at the molecular level, the collective data suggest that mMCP-6 and hTryptase-β are associated with macrophage accumulation and macrophage-dependent inflammation, remodeling, and emphysema in COPD.

DISCUSSION

COPD is a major respiratory health problem worldwide[2] that is usually caused by the chronic inhalation of cigarette smoke.[48,49] Although a heterogeneous disease, COPD is characterized by chronic airway inflammation (bronchitis) and/or emphysema, as well as reduced lung function.[49] The chronic inflammation that occurs in the smoke-exposed lung is thought to drive the progressive mucus hypersecretion, airway remodeling, and destruction of alveolar tissue that synergize to reduce pulmonary function.[48,49] While inhaled glucocorticoids and bronchodilators are used therapeutically to treat the symptoms and exacerbations of COPD,[39] there is no effective treatment that prevents the induction of the disease or halts its progression.[41]

The lack of a cigarette smoke-induced animal model of COPD of short duration that recapitulates the major features of the human condition has hindered our understanding of the disease. To address this deficiency, we developed a short-term mouse model of cigarette smoke-induced COPD that has most of the key pathological and clinical features of the human disease. Importantly, our *in vivo* model gradually progresses to overt disease over 6-8 weeks (Fig 1) and does not rapidly resolve (Fig 5). The hallmark features of the disease are induced within 8 weeks (Figs 1, 2, and S3), providing opportunities to identify therapeutic targets for both the induction and progression phases of the disease. As occurs in humans who smoke,[14,47,50] the direct delivery of smoke to the airways of WT BALB/c and B6 mice resulted in acute and chronic inflammation that

was dominated by neutrophils, macrophages, and eventually $CD8^+$ T cells (Figs 1 and S3). The disease also had a MC component (Figs 7 and 8).

Inflammation was associated with airway remodeling, emphysematous changes, and reduced lung function (Figs 1, 2, S2, and S3). The airway remodeling, alveolar enlargement and emphysema were likely due to inflammation-induced damage of the parenchymal walls. Together, the airway remodeling and emphysema in our model led to reduced lung function, as occurs in humans with COPD (Figs 2 and S3).

The only feature not consistent with human COPD was a decrease in airway resistance (Fig 2, *B* and *C*). This finding suggests an absence of obstruction despite the presence of goblet cell metaplasia and airway remodeling. Because mice have a greater proportion of parenchyma to airway tissue compared to humans, the reduced resistance might be the result of emphysema and associated reductions in tissue attachments. Alveolar distension and hyperinflation led to widening of the airways during ventilation and reduced resistance in other mouse models of emphysema.[51]

Glucocorticoids have limited efficacy in treating COPD symptoms in humans. They partially suppress chronic inflammation, but do not reverse the tissue lesions or modify factors that drive chronic disease, and have no effect on the decline in lung function.[40-42] As occurs in COPD patients, dexamethasone did not suppress inflammation, emphysema, or alterations in lung function in our model (Fig 3). COPD has a systemic component with changes in circulating leukocyte populations and loss of skeletal muscle mass.[43] Both of these features were observed in our model (Fig 4, *A* and *B*). COPD is also linked to cardiovascular disease, and the hearts of smoke-exposed WT mice had pathologic changes (Fig 4, *C*).

COPD patients have a 3-6 fold increased risk of *S. pneumoniae*-induced pneumonia.[52] They also are more susceptible to influenza virus and suffer more severe symptoms when infected.[53] Respiratory infections induce further inflammation and acute exacerbations of COPD symptoms which, in turn, increase the rate of disease progression.[54] The development of experimental COPD

was associated with enhanced respiratory infection by *S. pneumoniae* and influenza virus (Fig 4, *D* and *E*). The numbers of $CD8^+$ T cells that infiltrated the lungs of smoke-exposed mice were elevated but these lymphocytes had reduced expression of the activation marker CD98 (data not shown), which may contribute to impaired pathogen clearance. Although inflammation was increased, the latter findings suggest that immune function was suppressed, thereby predisposing the diseased mice to more severe pulmonary infections.

Once COPD develops in humans, the clinical condition and features of disease often deteriorate further even after the cessation of smoking.[2] After 8 weeks of smoking and 4 weeks of cessation in our model, macrophage accumulation in the airways of WT mice actually increased compared to that observed immediately after 8 weeks of smoking (Fig 5, *A*). It is possible that the increase in the number of macrophages in the lungs underpins the progression of COPD even after smoking cessation. This macrophage accumulation may be additionally exacerbated by infection that could further increase the rate of disease progression. There were no signs of resolution of any features of disease, at least 4 weeks after smoking cessation (Fig 5).

We then performed macrophage-depletion studies in WT mice to demonstrate that these phagocytes were essential for smoke-induced emphysema and reduced lung function (Fig 6). The clodronate method is the only method that can be used to reliably deplete the number of macrophages in the lungs of mice. Although clodronate might deplete some dendritic cells, there was no reduction in neutrophils by the method. Furthermore, the direct depletion of neutrophils did not suppress changes in lung structure or function (Fig S3).

The mechanisms that drive COPD pathogenesis are incompletely understood. Chronic influx of inflammatory cells into the lungs in COPD leads to the generation and release of pro-inflammatory cytokines, chemokines, and leukotrienes[55] that are thought to contribute to tissue destruction and the development of COPD. However, abnormalities in the protease:protease inhibitor balance in the lung also is important.[56] In that regard, MCs and their tryptase•serglycin proteoglycan complexes

promote inflammation in numerous diseases,[47,57,58] and MCs have been implicated in COPD pathogenesis.[13] MCs are common in inflammatory infiltrates in COPD, and increases in their numbers correlate with reduced lung function and airway remodeling.[14] The numbers of MCs detected in smoke-exposed mice were not high relative to other cell types (Fig 7). Nevertheless, it is well known that MCs release potent pro-inflammatory mediators, and that even small numbers of these cells can have devastating effects *in vivo* as occurs in systemic anaphylaxis.

hTryptase-β[59,60] comprises up to 50% of the protein content of a human MC. Its ortholog mMCP-6[61] has beneficial roles in the control of infections,[18,62] but adverse roles in MC-dependent inflammation of the airways,[53] joints,[47,57] and colon in mice.[58,63] However, the roles of MCs and their granule mediators in COPD pathogenesis have not been elucidated. In our model, there were no detectable increases in mMCP-6 mRNA or protein levels. This was not surprising since MC tryptases are pre-formed and stored in the cell's granules. Thus, changes in their mRNA levels are not as important as their release or the activation state of the MC. Only low levels of MCs were observed and mMCP-6 protein levels were below the limits of detection by immunoblot in whole lung tissues. There are no other more sensitive tests, such as ELISA, available. Nevertheless, Mortaz and coworkers, have demonstrated that cigarette smoke conditioned media induced the expression of mMCP-6 protein in primary cultured mast cells.[17]

Despite these data, the generation of mMCP-6$^{-/-}$ B6 mice[18] allowed us the opportunity for the first time to definitively evaluate the importance of this MC-restricted tryptase in experimental COPD. The MCs in WT BALB/c mice express mMCP-6[61] and the other tryptase family member mMCP-7.[64] In contrast, the MCs in WT B6 mice lack mMCP-7 due to a splice-site mutation in its gene.[65] The finding that all the features of COPD were similar in WT BALB/c (Fig 1) and B6 (Fig S3) mice indicates that mMCP-7 is not essential in our experimental model.

Smoke exposure resulted in enhanced pro-inflammatory cytokine and chemokine expression (Fig 1, *D-F* and 8, *E* and *F*) and increased the numbers of macrophages and MCs in the lungs of

WT B6 mice (Fig 7). We then employed our mMCP-6$^{-/-}$ B6 mice to demonstrate that the presence of this tryptase is required for smoke-induced pro-inflammatory cytokine and chemokine expression and accumulation of macrophages in the lung, and for airway epithelial thickening and emphysematous damage (Fig 8). There were no statistically significant differences between neutrophil numbers or chemokine mRNA levels in the lung (Fig 8, *C* and *F*) or the percentage of leukocytes that were neutrophils in the blood (data not shown) at baseline. Thus, the decreased cellular infiltration in the lungs of the smoke-treated mMCP-6-null mice was not due to a baseline defect. We then showed that recombinant hTryptase-β induced mouse macrophages to increase their expression of the transcripts that encode the cytokines and chemokines that are increased in the lungs of mice with experimental COPD. These findings suggest the tryptase contributes to COPD, at least in part, by directly activating the macrophages in the lungs of the diseased animals. Our discovery that macrophages and tryptase^{+} MCs participate in the pathogenesis of COPD in our model raise the possibility that these cells and their granule tetramer-forming tryptases have comparable adverse roles in human COPD. Thus, the next generation of hTryptase-β inhibitors might have efficacy in the treatment of patients with COPD.

In summary, we developed a short-term cigarette smoke-induced mouse model that has the hallmark features of COPD. This animal model enables the study of the pathogenesis of COPD in a significantly shorter time-frame than existing cigarette smoke-induced models, thereby providing opportunities for pharmacologic intervention. Our model also enables the evaluation of the consequences of COPD on the ability of the lung to combat infections. COPD is the result of a complex interplay of immune dysregulation, and our model allows the evaluation of other important parameters (e.g. systemic consequences) in COPD in the mouse. This study raises the possibility that macrophages and tryptase^{+} MCs might have similar adverse roles in patients with COPD.

REFERENCES

1. WHO. Global Burden of Disease: 2004 Update. 2008.

2. Rabe KF, Hurd S, Anzueto A, Barnes PJ, Buist SA, Calverley P, et al. Global strategy for the diagnosis, management, and prevention of chronic obstructive pulmonary disease: GOLD executive summary. Am J Respir Crit Care Med 2007:176:532-55.

3. Vlahos R, Bozinovski S, Gualano RC, Ernst M, Anderson GP. Modelling COPD in mice. Pulm Pharmacol Ther 2006:19:12-7.

4. Bracke KR, D'hulst AI, Maes T, Moerloose KB, Demedts IK, Lebecque S, et al. Cigarette smoke-induced pulmonary inflammation and emphysema are attenuated in CCR6-deficient mice. J Immunol 2006:177:4350-9.

5. Gaschler GJ, Zavitz CCJ, Bauer CMT, Skrtic M, Lindahl M, Robbins CS, et al. Cigarette smoke exposure attenuates cytokine production by mouse alveolar macrophages. Am J Respir Cell Mol Biol 2007:38:218-26.

6. Motz GT, Eppert BL, Wortham BW, Amos-Kroohs RM, Flury JL, Wesselkamper SC, et al. Chronic cigarette smoke exposure primes NK cell activation in a mouse model of chronic obstructive pulmonary disease. J Immunol 2010:184:4460-9.

7. Hodge S, Matthews G, Mukaro V, Ahern J, Shivam A, Hodge G, et al. Cigarette smoke-induced changes to alveolar macrophage phenotype and function are improved by treatment with procysteine. Am J Respir Cell Mol Biol 2011:44:673-81.

8. Atkinson JJ, Lutey BA, Suzuki Y, Toennies HM, Kelley DG, Kobayashi DK, et al. The role of matrix metalloproteinase-9 in cigarette smoke-induced emphysema. Am J Respir Crit Care Med 2011:183:876-84.

9. Hautamaki RD, Kobayashi DK, Senior RM, Shapiro SD. Requirement for macrophage elastase for cigarette smoke-induced emphysema in mice. Science 1997:277:2002-4.

10. Wright JL, Churg A. Smoking cessation decreases the number of metaplastic secretory cells in the small airways of the guinea pig. Inhal Toxicol 2002:14:1153-9.

11. Huvenne W, Pérez-Novo CA, Derycke L, De Ruyck N, Krysko O, Maes T, et al. Different regulation of cigarette smoke induced inflammation in upper versus lower airways. Respir Res 2010:11:100-9.

12. Ruwanpura SM, McLeod L, Miller A, Jones J, Bozinovski S, Vlahos R, et al. Interleukin-6 promotes pulmonary emphysema associated with apoptosis in mice. Am J Respir Cell Mol Biol 2011:45:720-30.

13. Mortaz E, Folkerts G, Redegeld F. Mast cells and COPD. Pulm Pharmacol Ther 2011:24:367-72.

14. Andersson CK, Mori M, Bjermer L, Lofdahl CG, Erjefalt JS. Alterations in lung mast cell populations in patients with chronic obstructive pulmonary disease. Am J Respir Crit Care Med 2010:181:206-17.

15. Ballarin A, Bazzan E, Zenteno RH, Turato G, Baraldo S, Zanovello D, et al. Mast cell infiltration discriminates between histopathological phenotypes of chronic obstructive pulmonary disease. Am J Respir Crit Care Med 2012:186:233-9.

16. Zhang X, Zheng H, Ma W, Wang F, Zeng X, Liu C, et al. Tryptase enzyme activity is correlated with severity of chronic obstructive pulmonary disease. Tohoku J Exp Med 2011:224:179-87.

17. Mortaz E, Givi ME, Da Silva CA, Folkerts G, Redegeld FA. A relation between TGF-β and mast cell tryptase in experimental emphysema models. Biochim Biophys Acta 2012:1822:1154-60.

18. Thakurdas SM, Melicoff E, Sansores-Garcia L, Moreira DC, Petrova Y, Stevens RL, et al. The mast cell-restricted tryptase mMCP-6 has a critical immunoprotective role in bacterial infections. J Biol Chem 2007:282:20809-15.

19. Thorburn AN, O'Sullivan BJ, Thomas R, Kumar RK, Foster PS, Gibson PG, et al. Pneumococcal conjugate vaccine-induced regulatory T cells suppress the development of allergic airways disease. Thorax 2010:65:1053-60.

20. Essilfie AT, Simpson JL, Horvat JC, Preston JA, Dunkley ML, Foster PS, et al. *Haemophilus influenzae* infection drives IL-17-mediated neutrophilic allergic airways disease. PLoS Pathog 2011:7:e1002244.

21. Preston JA, Essilfie AT, Horvat JC, Wade MA, Beagley KW, Gibson PG, et al. Inhibition of allergic airways disease by immunomodulatory therapy with whole killed *Streptococcus pneumoniae*. Vaccine 2007:25:8154-62.

22. Thorburn AN, Foster PS, Gibson PG, Hansbro PM. *Streptococcus pneumoniae* components suppress allergic airways disease and natural killer T cells by inducing regulatory T cells. J Immunol 2012:188:4611-20.

23. Horvat JC, Beagley KW, Wade MA, Preston JA, Hansbro NG, Hickey DK, et al. Neonatal chlamydial infection induces mixed T-cell responses that drive allergic airway disease. Am J Respir Crit Care Med 2007:176:556-64.

24. Starkey MR, Essilfie AT, Horvat JC, Kim RY, Nguyen DH, Beagley KW, et al. Constitutive production of IL-13 promotes early-life *Chlamydia* respiratory infection and allergic airway disease. Mucosal Immunol 2012: in press.

25. Li JJ, Wang W, Baines KJ, Bowden NA, Hansbro PM, Gibson PG, et al. IL-27/IFN-γ induce MyD88-dependent steroid-resistant airway hyperresponsiveness by inhibiting glucocorticoid signaling in macrophages. J Immunol 2010:185:4401-9.

26. Asquith KL, Horvat JC, Kaiko GE, Carey AJ, Beagley KW, Hansbro PM, et al. Interleukin-13 promotes susceptibility to chlamydial infection of the respiratory and genital tracts. PLoS Pathog 2011:7:e1001339.

27. Zhu M, Rhee I, Liu Y, Zhang W. Negative regulation of FcεRI-mediated signaling and mast cell function by the adaptor protein LAX. J Biol Chem 2006:281:18408-13.

28. Horvat JC, Starkey MR, Kim RY, Phipps S, Gibson PG, Beagley KW, et al. Early-life chlamydial lung infection enhances allergic airways disease through age-dependent differences in immunopathology. J Allergy Clin Immunol 2010:125:617-25.

29. Horvat JC, Starkey MR, Kim RY, Beagley KW, Preston JA, Gibson PG, et al. Chlamydial respiratory infection during allergen sensitization drives neutrophilic allergic airways disease. J Immunol 2010:184:4159-69.

30. Kumar RK, Herbert C, Kasper M. Reversibility of airway inflammation and remodelling following cessation of antigenic challenge in a model of chronic asthma. Clin Exp Allergy 2004:34:1796-802.

31. Harris RS. Pressure-volume curves of the respiratory system. Respir Care 2005:50:78-98.

32. Essilfie AT, Simpson JL, Dunkley ML, Morgan LC, Oliver BG, Gibson PG, et al. Combined *Haemophilus influenzae* respiratory infection and allergic airways disease drives chronic infection and features of neutrophilic asthma. Thorax 2012:67:588-99.

33. Preston JA, Beagley KW, Gibson PG, Hansbro PM. Genetic background affects susceptibility in nonfatal pneumococcal bronchopneumonia. Eur Respir J 2004:23:224-31.

34. Preston JA, Thorburn AN, Starkey MR, Beckett EL, Horvat JC, Wade MA, et al. *Streptococcus pneumoniae* infection suppresses allergic airways disease by inducing regulatory T-cells. Eur Respir J 2011:37:53-64.

35. Hsu AC, Barr I, Hansbro PM, Wark PA. Human influenza is more effective than avian influenza at antiviral suppression in airway cells. Am J Respir Cell Mol Biol 2011:44:906-13.

36. Hsu AC, Parsons K, Barr I, Lowther S, Middleton D, Hansbro PM, et al. Critical role of constitutive type I interferon response in bronchial epithelial cell to influenza infection. PLoS One 2012:7:e32947.

37. Daley JM, Thomay AA, Connolly MD, Reichner JS, Albina JE. Use of Ly6G-specific monoclonal antibody to deplete neutrophils in mice. J Leukoc Biol 2008:83:64-70.

38. Singh S, Amin AV, Loke YK. Long-term use of inhaled corticosteroids and the risk of pneumonia in chronic obstructive pulmonary disease: a meta-analysis. Arch Intern Med 2009:169:21929.

39. Calverley PM, Anderson JA, Celli B, Ferguson GT, Jenkins C, Jones PW, et al. Salmeterol and fluticasone propionate and survival in chronic obstructive pulmonary disease. N Engl J Med 2007:356:775-89.

40. Séguin RM, Ferrari N. Emerging oligonucleotide therapies for asthma and chronic obstructive pulmonary disease. Expert Opin Investig Drugs 2009:18:1505-17.

41. Yang IA, Fong KM, Sim EH, Black PN, Lasserson TJ. Inhaled corticosteroids for stable chronic obstructive pulmonary disease. Cochrane Database Syst Rev 2007:CD002991.

42. Barnes PJ. Glucocorticosteroids: current and future directions. Br J Pharmacol 2011:163:29-43.

43. Barnes PJ, Celli BR. Systemic manifestations and comorbidities of COPD. Eur Respir J 2009:33:1165-85.

44. Miravitlles M, Marín A, Monsó E, Vilà S, de la Roza C, Hervás R, et al. Colour of sputum is a marker for bacterial colonisation in chronic obstructive pulmonary disease. Respir Res 2010:11:58-67.

45. Morris DG, Huang X, Kaminski N, Wang Y, Shapiro SD, Dolganov G, et al. Loss of integrin $\alpha_v\beta_6$-mediated TGF-β activation causes MMP12-dependent emphysema. Nature 2003:422:169-73.

46. Ofulue AF, Ko M, Abboud RT. Time course of neutrophil and macrophage elastinolytic activities in cigarette smoke-induced emphysema. Am J Physiol 1998:275:L1134-44.

47. McNeil HP, Shin K, Campbell IK, Wicks IP, Adachi R, Lee DM, et al. The mouse mast cell-restricted tetramer-forming tryptases mouse mast cell protease 6 and mouse mast cell protease 7 are critical mediators in inflammatory arthritis. Arthritis Rheum 2008:58:2338-46.

48. Houghton AM, Mouded M, Shapiro SD. Common origins of lung cancer and COPD. Nat Med 2008:14:1023-4.

49. Hogg JC. Pathophysiology of airflow limitation in chronic obstructive pulmonary disease. Lancet 2004:364:709-21.

50. Battaglia S, Mauad T, van Schadewijk AM, Vignola AM, Rabe KF, Bellia V, et al. Differential distribution of inflammatory cells in large and small airways in smokers. J Clin Pathol 2007:60:907-11.

51. Vanoirbeek JA, Rinaldi M, De Vooght V, Haenen S, Bobic S, Gayan-Ramirez G, et al. Noninvasive and invasive pulmonary function in mouse models of obstructive and restrictive respiratory diseases. Am J Respir Cell Mol Biol 2010:42:96-104.

52. Welte T, Köhnlein T. Global and local epidemiology of community-acquired pneumonia: the experience of the CAPNETZ Network. Semin Respir Crit Care Med 2009:30:127-35.

53. Seemungal T, Harper-Owen R, Bhowmik A, Moric I, Sanderson G, Message S, et al. Respiratory viruses, symptoms, and inflammatory markers in acute exacerbations and stable chronic obstructive pulmonary disease. Am J Respir Crit Care Med 2001:164:1618-23.

54. Wilkinson TM, Patel IS, Wilks M, Donaldson GC, Wedzicha JA. Airway bacterial load and FEV_1 decline in patients with chronic obstructive pulmonary disease. Am J Respir Crit Care Med 2003:167:1090-5.

55. Keatings VM, Collins PD, Scott DM, Barnes PJ. Differences in interleukin-8 and tumor necrosis factor-α in induced sputum from patients with chronic obstructive pulmonary disease or asthma. Am J Respir Crit Care Med 1996:153:530-4.

56. Keely S, Talley NJ, Hansbro PM. Pulmonary-intestinal crosstalk in mucosal inflammatory disease. Mucosal Immunol 2012:5:7-18.

57. Shin K, Nigrovic PA, Crish J, Boilard E, McNeil HP, Larabee KS, et al. Mast cells contribute to autoimmune inflammatory arthritis via their tryptase/heparin complexes. J Immunol 2009:182:647-56.

58. Hamilton MJ, Sinnamon MJ, Lyng GD, Glickman JN, Wang X, Xing W, et al. Essential role for mast cell tryptase in acute experimental colitis. Proc Natl Acad Sci U S A 2011:108:290-5.

59. Schwartz LB, Lewis RA, Austen KF. Tryptase from human pulmonary mast cells. Purification and characterization. J Biol Chem 1981:256:11939-43.

60. Miller JS, Moxley G, Schwartz LB. Cloning and characterization of a second complementary DNA for human tryptase. J Clin Invest 1990:86:864-70.

61. Reynolds DS, Stevens RL, Lane WS, Carr MH, Austen KF, Serafin WE. Different mouse mast cell populations express various combinations of at least six distinct mast cell serine proteases. Proc Natl Acad Sci U S A 1990:87:3230-4.

62. Shin K, Watts GF, Oettgen HC, Friend DS, Pemberton AD, Gurish MF, et al. Mouse mast cell tryptase mMCP-6 is a critical link between adaptive and innate immunity in the chronic phase of *Trichinella spiralis* infection. J Immunol 2008:180:4885-91.

63. Oh SW, Pae CI, Lee DK, Jones F, Chiang GK, Kim HO, et al. Tryptase inhibition blocks airway inflammation in a mouse asthma model. J Immunol 2002:168:1992-2000.

64. McNeil HP, Reynolds DS, Schiller V, Ghildyal N, Gurley DS, Austen KF, et al. Isolation, characterization, and transcription of the gene encoding mouse mast cell protease 7. Proc Natl Acad Sci U S A 1992:89:11174-8.

65. Hunt JE, Stevens RL, Austen KF, Zhang J, Xia Z, Ghildyal N. Natural disruption of the mouse mast cell protease 7 gene in the C57BL/6 mouse. J Biol Chem 1996:271:2851-5.

FIGURE LEGENDS

FIG 1. Nose-only exposure of the lungs of BALB/c mice to cigarette smoke induces the hallmark features of human COPD. **A-I**, WT BALB/c mice were exposed to cigarette smoke or normal air for 1-12 weeks. Relative to control mice, smoke-exposed mice had (**A**) reduced weight-gain relative to initial weight; (**B**) acute (after 4 days) and chronic (after 8 weeks) increases in the numbers of macrophages (M), neutrophils (N) and lymphocytes (L) in BALF; (**C**) increased cellular infiltrates in the parenchyma; increased levels of the transcripts that encode (**D**) TNF-α, (**E**) Cxcl1, and (**F**) IL-1β in lung homogenates; (**G**) increased number of mucus-secreting goblet cells (MSCs) in the airways; (**H**) airway epithelium thickening; and (**I**) alveolar enlargement (scale bar on micrographs = 100 μm). Data are means±SEM of 6-8 mice/group, # $P<0.05$, ## $P<0.01$, ### $P<0.001$ compared to mice that breathed normal air, * $P<0.05$, ** $P<0.01$ compared to other groups indicated. Statistical significance of the reduced weight gain is for the whole curve.

FIG 2. Nose-only cigarette smoke exposure leads to changes in lung function that are similar to that in humans with COPD. **A-I**, WT BALB/c mice were exposed to cigarette smoke or normal air for 8 weeks. Relative to control mice, smoke-exposed mice had decreased (**A**) hysteresis, (**B**) transpulmonary and (**C**) airway-specific resistance (RI) and (**D**) tissue damping, but increased (**E**) dynamic compliance (Cdyn), (**F**) work of breathing, (**G**) functional residual capacity (FRC), and (**H**) total lung capacity (TLC), and (**I**) reduced ratio of forced expiratory volume in 100 milliseconds/forced vital capacity (FEV_{100}/FVC). Data are means±SEM of 6-8 mice/group, # $P<0.05$, compared to mice that breathed normal air.

FIG 3. Experimental COPD is glucocorticoid-resistant. **A-F**, WT BALB/c mice were exposed to cigarette smoke or normal air for 12 weeks and were treated with dexamethasone or sham-treated

with sterile distilled water either prophylactically throughout (Dex), or therapeutically (tDex) for the last 6 weeks, of the smoking protocol. Steroid treatment had no effect on (**A**) macrophage (M), neutrophil (N) and lymphocyte (L) numbers in the BALF, (**B**) alveolar enlargement or changes in lung function; (**C**) work of breathing, (**D**) total lung capacity (TLC), (**E**) functional residual capacity (FRC) or (**F**) forced expiratory volume in 100 milliseconds/forced vital capacity (FEV_{100}/FVC) ratio. Data are means±SEM of 6-8 mice/group, # P<0.05, ## P<0.01, ### P<0.001 compared to mice that breathed normal air. There were no differences between other groups.

FIG 4. Experimental COPD has systemic involvement and exacerbates respiratory infections. **A-E**, WT BALB/c mice were exposed to cigarette smoke or normal air for 8 weeks. Relative to control mice, smoke-exposed mice had (**A**) alterations in the proportions of monocytes (M, decreased), neutrophils (N, increased), and lymphocytes (L, increased) in blood; (**B**) reduced quadriceps weight; (**C**) increased heart weight, size, and fatty deposits; and decreased (**D**) clearance of *S. pneumoniae* (after 48 hours of infection) and (**E**) influenza virus (after 7 days of infection). Data are means±SEM of 6-8 mice/group, # P<0.05, ## P<0.01, compared to WT mice that breathed normal air.

FIG 5. Experimental COPD does not rapidly resolve following cessation of smoke exposure. **A-F**, WT BALB/c mice were exposed to cigarette smoke or normal air for 8 weeks. Smoke exposed mice were evaluated immediately after the cessation of smoking or 4 weeks later. Relative to control mice, both groups of smoke-exposed mice had (**A**) increased airway inflammation; (**B**) alveolar enlargement; and changes in lung function; decreased (**C**) transpulmonary and (**D**) airway-specific resistance (RI); (**E**) increased dynamic compliance (Cdyn); as well as (**F**) altered leukocyte populations in blood. Mice that had ceased smoking 4 weeks earlier had more macrophages, but fewer neutrophils, in their BALF. Data are means±SEM

of 6-8 mice/group, # $P<0.05$, ## $P<0.01$, compared to mice that breathed normal air, * $P<0.05$, compared to other groups indicated.

FIG 6. Depletion of pulmonary macrophages suppresses the development of experimental COPD. **A-E**, WT BALB/c mice were exposed to cigarette smoke or normal air for 8 weeks. These two groups of mice also were treated with either liposome encapsulated clodronate or empty liposomes (Sham) 3 times/week for the duration of the experiment commencing on the 1st day of smoking. Relative to smoke-exposed macrophage-sufficient mice, smoke-exposed macrophage-depleted mice had reduced (**A**) airway epithelium thickening; and (**B**) alveolar enlargement; and altered lung function; increased (**C**) transpulmonary and (**D**) increased airway-specific resistance (RI), and (**E**) reduced dynamic compliance (Cdyn). The smoke-exposed macrophage-depleted mice had no alveolar enlargement or changes in lung function compared to non-smoke exposed control mice. Data are means±SEM of 6-8 mice/group, ## $P<0.01$, ### $P<0.001$ compared to mice that breathed normal air, * $P<0.05$, ** $P<0.01$ *** $P<0.001$ compared to other groups indicated.

FIG 7. Experimental COPD increases the numbers of pulmonary macrophages and MCs. **A-C**, WT B6 mice were exposed to cigarette smoke or normal air for 8 weeks. Some mice were then rested for 4 weeks after smoking. Other mice were treated with clodronate. Relative to control mice, smoke-exposed mice had increased numbers of (**A**) F4/80$^+$ macrophages and (**B**) Kit$^+$/FcεRI$^+$/IgE$^+$ (by flow cytometry in the largest lobe of the multi-lobed right lung) or (**C**) toluidine blue$^+$ (by histochemistry in the single-lobed left lung) MCs in the lungs. Smoking cessation did not alter macrophage or MC numbers. Clodronate specifically attenuated macrophage numbers. Data are means±SEM of 6-8 mice/group, # $P<0.05$, compared to mice that breathed normal air.

FIG 8. The tryptase mMCP-6 contributes to pulmonary macrophage accumulation and parenchymal inflammation, and is required for airway remodeling and alveolar enlargement in experimental COPD. **A-J**, WT and mMCP-$6^{-/-}$ B6 mice were exposed to cigarette smoke or normal air for 8 weeks. Relative to smoke-exposed WT mice, smoke-exposed mMCP-$6^{-/-}$ mice had (**A**) no change in the number of Kit^{+}/$Fc\varepsilon RI^{+}$/IgE^{+} MCs but had reduced (**B**) numbers of $F4/80^{+}$ macrophages and (**C**) neutrophils in the lung, (**D**) less cellular infiltrates in the parenchyma, attenuated (**E**) TNF-α and (**F**) Cxcl1 mRNA levels in lung homogenates, (**G**) diminished alveolar enlargement, (**H**) no airway remodelling and no differences in lung function [e.g. (**I**) transpulmonary resistance (RI) or (**J**) dynamic compliance (Cdyn)]. **K-M**, B6 mouse bone marrow-derived macrophages were cultured in the absence or presence of recombinant hTryptase-β. Relative to untreated cells, hTryptae-β-treated cells had increased levels of the transcripts that encode (**K**) TNF-α, (**L**) Cxcl1 and (**M**) IL-1β. Data are means±SEM of 6-8 mice/group, or of 3 cell cultures in triplicate (representative of 4 repeat experiments), # $P<0.05$, ## $P<0.01$, ### $P<0.001$ compared to mice that breathed normal air (**A-J**) or compared to sham-treated macrophages (**K-M**), * $P<0.05$, compared to other groups indicated.

A short-term model of COPD identifies a role for mast cell tryptase

Online Repository

SUPPORTING INFORMATION

Mice

All mice were female and 6-8 weeks of age at the commencement of each experiment. Mouse mast cell (MC) protease (mMCP)-6$^{-/-}$ C57BL/6 (B6) mice were previously described.[E1] WT and mMCP-6$^{-/-}$ mice were housed in the same animal facility at The University of Newcastle. All mice received the same diets. Mice were euthanized by intraperitoneal sodium pentobarbital overdose. All animal experiments were approved by the animal ethics committee of The University of Newcastle.

Smoke exposure

Nose-only exposure was achieved using specialized containment tubes that delivered smoke and normal air directly to the animal's nose. This protocol allowed a more intensive delivery of smoke than whole body exposure systems. For the first 2 days, mice were exposed to one session of smoking with 12 puffs from each cigarette to allow acclimatization. Smoke was delivered in 2-second puffs, with 30 seconds of normal air between each puff. After day 2, the mice were subjected to two sessions in which they were exposed to the smoke from 12 cigarettes (morning and afternoon, separated by a recovery period). Despite the intensive exposure, no deaths due to acute toxicity were observed. Age-matched control mice breathed normal air for the same periods of time (i.e., 4, 6, 8, or 12 weeks). The dose of smoke was determined by performing acute (4 days)

dose-response experiments using different levels of smoke exposure. The dose selected induced acute neutrophilic inflammation without inducing overt toxicity in exposed mice.

Airway and lung inflammation

Airway inflammation was assessed by staining cytospins of cells in bronchoalveolar lavage fluid (BALF) (two 0.8 mL washes with phosphate buffered saline) with May Grunwald-Geimsa, and then enumeration of the different inflammatory cell types using light microscopy, as previously described.[E2-4] Total cell numbers were determined (cells/mL) using Trypan blue staining and a hemocytometer. Parenchymal inflammation was assessed by hematoxylin and eosin staining and counting the inflammatory cells in 10 randomized fields (selected from a pool of 50, x100 magnification).[E5] The results for the 10 fields were averaged to produce the results for each mouse.

Transcript expression in the lung

Single cell suspensions of whole lungs were digested with collagenase D and homogenized using a gentleMACS Dissociator (Miltenyi Biotec, Sydney, Australia). Total RNA was extracted from homogenized lungs using Trizol Reagent (Invitrogen, Life Technologies Ltd, Paisley, UK), and first strand cDNA was synthesized using oligo(dT)-primed reverse transcription with Superscript II (Invitrogen), according to the manufacturer's instructions.[E6] Real-time quantitative real-time polymerase chain reaction (qPCR) assays were performed using SYBR Green Supermix (KAPA Biosystems, Tharburton, Australia) and a ViiA7 thermal cycler (Life Technologies, Carlsbad, Calif). mRNA levels were normalized to that of the transcript that encodes the house-keeping protein hypoxanthine-guanine phosphoribosyl transferase (HPRT).[E6] The primers used in these qPCR assays are listed in Supplementary Table 1.

Airway remodeling

The thickness of the airway epithelium was calculated by measuring the difference between the area encompassing the epithelial cell basement membrane and lumen, and was expressed as the epithelial area. Measurements were obtained using Image Pro Plus. The numbers of mucus^{+} goblet cells around the airways were determined and expressed as a percent change from that in control mice.[E4-7] This prevents the size of the airways from impacting the results. Only whole, round, non-cartilaginous airways were selected to prevent the angle of cut producing spurious results.[E8] These analyses were conducted in a blinded fashion.

Emphysema

Emphysema was assessed using the mean linear intercept technique.[E6] Following exsanguination, lungs were perfused with 0.9% saline under the pressure of 40 cm H_2O for 60 seconds to remove excess blood from the pulmonary capillary bed. The trachea was cannulated using a blunted 19-gauge needle. The lungs were then gently inflated with 10% buffered formalin (1 mL), and then immersed in 10% buffered formalin. Fixed volume inflation was chosen as it has been shown to maintain lung architecture and simultaneously prevents over-inflation of the lung, which would artificially enhance any increase in alveolar size in mice with signs of emphysema.[E9] Lungs were embedded in paraffin, and 5 μm sections were stained with hematoxylin and eosin for histological analysis. Fifty randomized photomicrographs from 3 stained sections per mouse were obtained using a light microscope and digital camera linked to image analysis software (Image Pro Plus, version 6.0). The first 10 randomly selected photos that were free of cutting artifacts, compression, large airways or blood vessels were used for analysis. An 11-horizontal line overlay was applied to each image, and the average alveolar diameter was calculated by dividing the total length of these lines by the number of alveolar wall intercepts. The results from each of the 10

photomicrographs that were counted were then averaged to give a result per mouse. All histological analysis was conducted in a blinded fashion.

Lung function

Mice were anesthetized with ketamine (100 mg/kg) and xylazine (10 mg/kg). They were then cannulated (tracheostomy with ligation).[E4,E5,E10] Flexivent apparatus (Legacy system, SCIREQ, Montreal, Canada) was used to assess hysteresis, transpulmonary resistance and compliance, tissue damping and airway-specific resistance at baseline (using a tidal volume of 8 mL/kg at a respiratory rate of 450 breaths/minute). This combination of anesthesia and ventilation is common and recommended by the manufacturer.[E11,E12] Maximal pressure/volume (PV) loops were used to calculate hysteresis.[E13] Transpulmonary resistance and dynamic compliance were assessed using the snapshot perturbation function. The forced oscillation perturbation was then used to determine the airway's (Newtonian) resistance and tissue damping. For all perturbations, a coefficient of determination of 0.95 was the minimum allowable for an acceptable measurement. Each perturbation was conducted 3 times per animal and the average calculated, with a minimum ventilation period of 20 seconds allowed between each perturbation. Work of breathing, functional residual capacity (FRC), total lung capacity (TLC), forced expiratory volume at 100 milliseconds (FEV_{100}), and functional vital capacity (FVC) were measured using a forced pulmonary maneuver system (Buxco, Wilmington, Nc). An average breathing frequency of 150 breaths/minute was applied to anesthetized animals. Work of breathing and TLC were determined using the quasistatic PV-loop, FRC was determined using the Boyles Law FRC maneuver, and FEV_{100} and FVC were calculated using the fast-flow maneuver. Each maneuver was performed a minimum of 3 times, and the average calculated.

Respiratory infections

Mice were infected with mouse-adapted strains of *Streptococcus pneumoniae* [$2x10^6$ colony forming units (CFUs), intratracheally, D39 strain, serotype 2] or influenza virus [8 plaque forming units (PFUs), intranasally, A/PR/8 H1N1 strain]. Whole lungs were homogenized, and pathogen loads in CFUs or PFUs were determined by culture plating and enumeration[E14,E15] or plaque assay,[E16,E17] respectively. For intratracheal administration, mice were anesthetized with 10 mg/kg alfaxan by the intravenous route. For intranasal administration, mice were anesthetized with inhaled gaseous isoflurane (3-5%).

Macrophage depletion

Clodronate was a gift from Roche Diagnostics GmbH, Mannheim, Germany.[E11] It was encapsulated in liposomes using phosphatidylcholine (LIPOID E PC, Lipoid GmbH, Ludwigshafen, Germany) and cholesterol (Sigma Chemicals, Sydney Australia). The resulting preparations were stored under nitrogen gas, and 50 μL aliquots were administered intranasally, under anesthesia to each animal 3 times per week. Sham inoculated mice received empty liposomes.

Neutrophil depletion

Neutrophils were depleted by intraperitoneal injection of anti-Ly6G antibody (500 μg, 1A8, Bioxcell, Lebannon, USA) administered in 200 μl saline 3 times per week for the duration of smoke exposure.[E18] Sham control mice received isotype antibody (IgG2A, 2A39, Bioxcell).

Flow cytometry analysis for macrophages, MCs and neutrophils

Macrophages, MCs, and neutrophils were identified based on their surface expression of the F4/80/Emr1 antigen, Kit/CD117/FcεRI/IgE, and CD11b/Gr-1, respectively.[E11,E18,E19,] The antibodies used in these immunohistochemistry assays were obtained from BioLegend (San Diego,

Calf). Total cell numbers in homogenates of single lung lobes were enumerated using Trypan blue staining and a hemocytometer. The obtained data were then used to convert the percentage populations identified by flow cytometry to the numbers of cells per large lung lobe.

MC immunohistochemistry

Paraffin-embedded tissue sections were mounted on glass slides. Slides were deparaffinized through a series of xylene and ethanol washes and then hydrated with distilled water. Slides were treated with Toluidine blue (0.1% in 1% NaCl, Sigma) for 2.5 min. They were rinsed in distilled water 3 times, dehydrated quickly through 95% and absolute alcohol, exposed to xylene, and coverslipped. Metrochromatic stained cells were enumerated in sections of the largest lobe of the multi-lobed lung ($n \geq 6$-8 per group).[E20]

SDS-PAGE immunoblot analysis of mMCP-6 protein

Protein lysates were prepared from frozen lung tissues, which were homogenized in radio-immunoprecipitation assay (Sigma) lysis buffer supplemented with complete mini protease inhibitor tablets and PhosStop phosphatase inhibitor tablets (Roche, Indianapolis, In). Lysates were cleared of debris and concentrated by centrifugation (40 minutes, 3,000 x*g*, Amicon Ultra 4, 10,000 MW cut-off, Millipore). The soluble proteins were separated by 12.5% SDS-PAGE, and then transferred to a PVDF membrane using a wet transfer system (Mini Trans-Blot Cell, Bio-Rad, Hercules, Calif). The resulting membrane was blocked (5% bovine serum albumin, Sigma), and then incubated with rat monoclonal anti-mMCP-6 antibody MAB3736 (R&D, Minneapolis, Mn) followed by horseradish peroxidase-conjugated anti-rat IgG antibody HAF005 (R&D). Immunoreactive mMCP-6 was visualized by enhanced chemiluminescence (ChemiDoc, Biorad).

Transcript expression in tryptase-treated macrophages

Primary non-transformed macrophages were generated by culturing B6 mouse bone marrow cells for 7 days in α-modified essential medium (Gibco/Life Technologies-Invitrogen, Carlsbad, Calif) supplemented with ribonucleosides, penicillin, streptomycin, 10% heat-inactivated fetal calf serum (Hyclone Lab., Logan, Ut), and 10% conditioned medium obtained from the mouse macrophage-colony stimulating factor-expressing cell line CMG14-12.[E21,E22] Before each experiment, the conditioned medium was removed, and the resulting plastic-adherent macrophages in each 12-well plate (~100,000 macrophages/well) were cultured for an additional 18 hours in the fresh medium containing 1% fetal calf serum (rather than 10% fetal calf serum) in the absence or presence of recombinant hTryptase-β (0.8 μg/ml, 25 nM, Promega, Madison, Wi). RNeasy mini kits (Qiagen) were used to isolate RNA, which was then converted into cDNA using iScript cDNA synthesis kits (Bio-Rad Lab., Hercules, Calif). Employing Qiagen's validated primer sets and a Stratagene Mx3000P system, qPCR assays were used to evaluate the levels of the transcripts that encode tumor necrosis factor-α (TNF-α), Cxcl1/keratinocyte chemokine (KC), and interleukin (IL)-1β. The transcript that encodes glyceraldehyde 3-phosphate dehydrogenase was used as the positive reference control. All qPCR assays were performed with SYBR green reagents.

SUPPLEMENTAL REFERENCES

E1. Thakurdas SM, Melicoff E, Sansores-Garcia L, Moreira DC, Petrova Y, Stevens RL, et al. The mast cell-restricted tryptase mMCP-6 has a critical immunoprotective role in bacterial infections. J Biol Chem 2007:282:20809-15.

E2. Thorburn AN, O'Sullivan BJ, Thomas R, Kumar RK, Foster PS, Gibson PG, et al. Pneumococcal conjugate vaccine-induced regulatory T cells suppress the development of allergic airways disease. Thorax 2010:65:1053-60.

E3. Essilfie AT, Simpson JL, Horvat JC, Preston JA, Dunkley ML, Foster PS, et al. *Haemophilus influenzae* infection drives IL-17-mediated neutrophilic allergic airways disease. PLoS Pathog 2011:7:e1002244.

E4. Thorburn AN, Foster PS, Gibson PG, Hansbro PM. *Streptococcus pneumoniae* components suppress allergic airways disease and natural killer T cells by inducing regulatory T cells. J Immunol 2012:188:4611-20.

E5. Horvat JC, Beagley KW, Wade MA, Preston JA, Hansbro NG, Hickey DK, et al. Neonatal chlamydial infection induces mixed T-cell responses that drive allergic airway disease. Am J Respir Crit Care Med 2007:176:556-64.

E6. Horvat JC, Starkey MR, Kim RY, Phipps S, Gibson PG, Beagley KW, et al. Early-life chlamydial lung infection enhances allergic airways disease through age-dependent differences in immunopathology. J Allergy Clin Immunol 2010:125:617-25.

E7. Kumar RK, Herbert C, Kasper M. Reversibility of airway inflammation and remodelling following cessation of antigenic challenge in a model of chronic asthma. Clin Exp Allergy 2004:34:1796-802.

E8. O'Reilly M, Hooper SB, Allison BJ, Flecknoe SJ, Snibson K, Harding R, et al. Persistent bronchiolar remodeling following brief ventilation of the very immature ovine lung. Am J Physiol Lung Cell Mol Physiol 2009:297:L992-1001.

E9. Braber S, Verheijden KA, Henricks PA, Kraneveld AD, Folkerts G. A comparison of fixation methods on lung morphology in a murine model of emphysema. Am J Physiol Lung Cell Mol Physiol 2010:299:L843-51.

E10. Preston JA, Essilfie AT, Horvat JC, Wade MA, Beagley KW, Gibson PG, et al. Inhibition of allergic airways disease by immunomodulatory therapy with whole killed *Streptococcus pneumoniae.* Vaccine 2007:25:8154-62.

E11. Li JJ, Wang W, Baines KJ, Bowden NA, Hansbro PM, Gibson PG, et al. IL-27/IFN-γ induce MyD88-dependent steroid-resistant airway hyperresponsiveness by inhibiting glucocorticoid signaling in macrophages. J Immunol 2010:185:4401-9.

E12. Harris RS. Pressure-volume curves of the respiratory system. Respir Care 2005; 50:78-98.

E13. Bedoret D, Wallemacq H, Marichal T, Desmet C, Quesada Calvo F, Henry E, et al. Lung interstitial macrophages alter dendritic cell functions to prevent airway allergy in mice. J Clin Invest 2009:119:3723-38.

E14. Preston JA, Beagley KW, Gibson PG, Hansbro PM. Genetic background affects susceptibility in nonfatal pneumococcal bronchopneumonia. Eur Respir J 2004:23:224-31.

E15. Preston JA, Thorburn AN, Starkey MR, Beckett EL, Horvat JC, Wade MA, et al. *Streptococcus pneumoniae* infection suppresses allergic airways disease by inducing regulatory T-cells. Eur Respir J 2011:37:53-64.

E16. Hsu AC, Barr I, Hansbro PM, Wark PA. Human influenza is more effective than avian influenza at antiviral suppression in airway cells. Am J Respir Cell Mol Biol 2011:44:906-13.

E17. Hsu AC, Parsons K, Barr I, Lowther S, Middleton D, Hansbro PM, et al. Critical role of constitutive type I interferon response in bronchial epithelial cell to influenza infection. PLoS One 2012:7:e32947.

E18. Daley JM, Thomay AA, Connolly MD, Reichner JS, Albina JE. Use of Ly6G-specific monoclonal antibody to deplete neutrophils in mice. J Leukoc Biol 2008:83:64-70.

E19. Asquith KL, Horvat JC, Kaiko GE, Carey AJ, Beagley KW, Hansbro PM, et al. Interleukin-13 promotes susceptibility to chlamydial infection of the respiratory and genital tracts. PLoS Pathog 2011:7:e1001339.

E20. Zhu M, Rhee I, Liu Y, Zhang W. Negative regulation of FcεRI-mediated signaling and mast cell function by the adaptor protein LAX. J Biol Chem 2006:281:18408-13.

E21. Warren MK, Vogel SN. Bone marrow-derived macrophages: development and regulation of differentiation markers by colony-stimulating factor and interferons. J Immunol 1985:134:982-9.

E22. Takeshita S, Kaji K, Kudo A. Identification and characterization of the new osteoclast progenitor with macrophage phenotypes being able to differentiate into mature osteoclasts. J Bone Miner Res 2000:15:1477-88.

SUPPLEMENTAL FIGURE LEGENDS

FIG S1. Custom-designed and purpose-built directed flow inhalation and smoke-exposure system. **A-C**, (**A**) Smoking apparatus, (**B**) a mouse in one of the smoking chambers, and (**C)** smoking cigarette.

FIG S2. Depletion of pulmonary neutrophils does not suppress the development of experimental COPD. **A-E**, WT BALB/c mice were exposed to cigarette smoke or normal air for 8 weeks. The two groups of mice also were treated with either anti-Ly6G antibody or isotype control antibody (Sham) 3 times per week for the duration of the experiment commencing on the first day of smoking. Relative to smoke-exposed macrophage-sufficient mice, neutrophil depletion had no effect on (**A**) alveolar enlargement, or alterations in lung function; (**B**) transpulmonary or (**S**) airway-specific resistance (RI), or (**D**) dynamic compliance (Cdyn). Data are means±SEM of 6-8 mice/group, ## $P<0.01$, ### $P<0.001$ compared to mice that breathed normal air.

FIG S3. Nose-only exposure of WT C57BL/6 mice to cigarette smoke induces the hallmark features of human COPD. **A-N**, WT C57BL/6 mice were exposed to cigarette smoke or normal air for 8 weeks. Relative to control mice, smoke-exposed mice had (**A**) reduced weight gain relative to initial weight; increased (**B**) cellular infiltrates in the parenchyma and (**C**) number of mucus-secreting goblet cells (MSCs) around the airways; (**D**) airway epithelium thickening; (**E**) alveolar enlargement; and reduced lung function; decreased (**F**) hysteresis, (**G**) transpulmonary and (**H**) airway resistance (RI) and (**I**) tissue damping; increased (**J**) dynamic compliance (Cdyn), (**K**) difficulty of breathing, (**L**) functional residual capacity (FRC) and (**M**) total lung capacity (TLC); and (**N**) reduced ratio of forced expiratory volume in 100 milliseconds/forced

vital capacity (FEV_{100}/FVC). Data are the mean±SEM of 6-8 mice/group, # $P<0.05$, ## $P<0.01$, ### $P<0.001$ compared to mice that received normal air. Statistical significance of the reduced weight gain is for the whole curve.

FIG S4. Histograms showing the gating strategy used to identify (**A**) macrophages and (**B**) MCs in whole lung homogenates by flow cytometry.

SUPPLEMENTARY TABLE S1

Primer	Nucleotide Sequence
Cxcl1 Forward	5'-GCTGGGATTCACCTCAAGAA-3'
Cxcl1 Reverse	5'-CTTGGGGACACCTTTTAGCA-3'
HPRT Forward	5'-AGGCCAGACTTTGTTGGATTTGAA-3'
HPRT Reverse	5'-CAACTTGCGCTCATCTTAGGCTTT-3'
IFN-γ Forward	5'-GAGGAACTGGCAAAAGG-3'
IFN-γ Reverse	5'-TTGCTGATGGCCTGATTGTC-3'
IL-1β Forward	5'-TGGGATCCTCTCCAGCCAAGC-3'
IL-1β Reverse	5'-AGCCCTTCATCTTTTGGGGTCCG-3'
IL-6 Forward	5'-AGAAAACAATCTGAAACTTC CAGAGAT-3'
IL-6 Reverse	5'-GAAGACCAGAGGAAATTTTCAATAGG-3'
IL-10 Reverse	5'-GCCTTGTAGACACCTTGGTCTTGG-3'
IL-13 Forward	5'-CAGCCTCCCCGATACCAAAAT-3'
IL-13 Reverse	5'-GCGAAACAGTTGCTTTGTGTAG-3'
mMCP-6 Forward	5'-CATTTCTGCGCGCAGGTTCTCTC-3'
mMCP-6 Reverse	5'-CACCACGATCCTGTTCAAAGA-3'
TNF-α Forward	5'-TCTGTCTACTGAACTTCGGGGTGA-3'
TNF-α Reverse	5'-TTGTCTTTGAGATCCATGCCGTT-3'

A

B

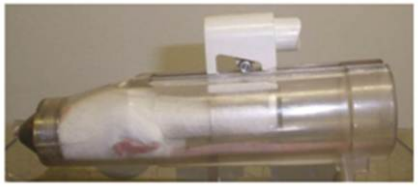

C

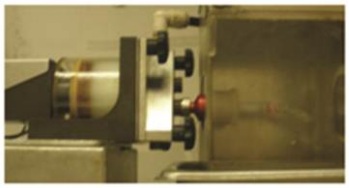

Supplementary figure 1

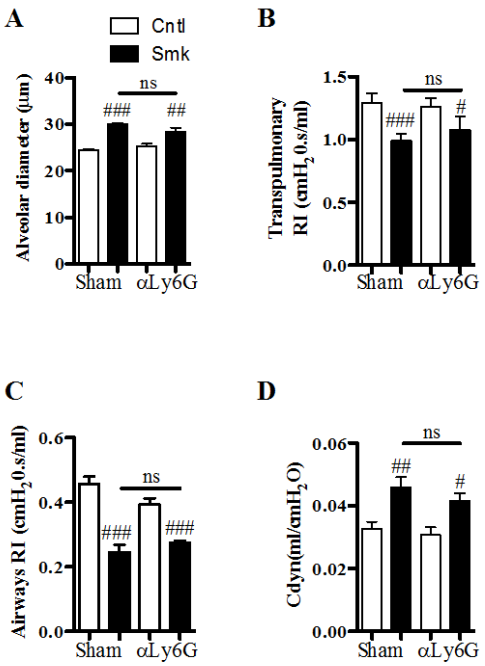

SUPPLEMENTARY FIGURE 2

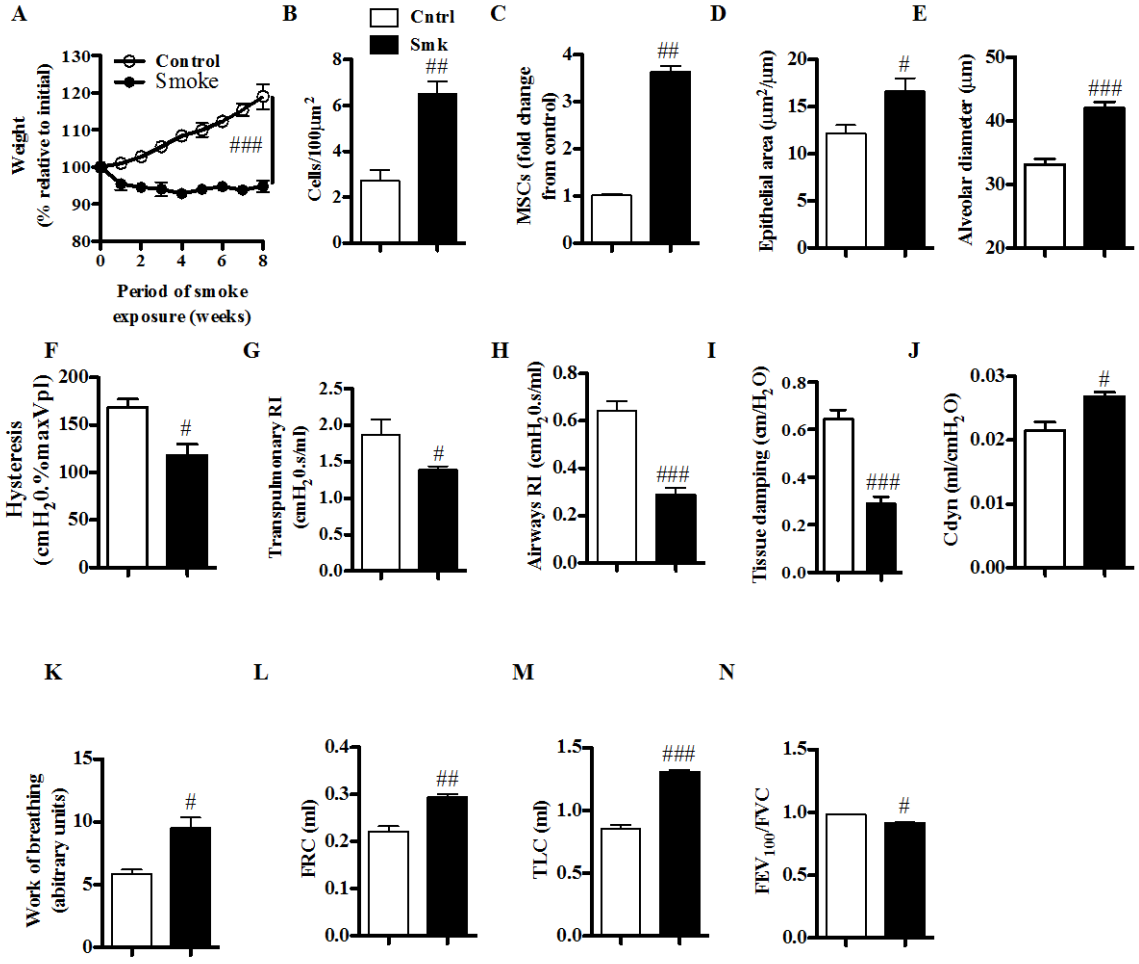

SUPPLEMENTARY FIGURE 3

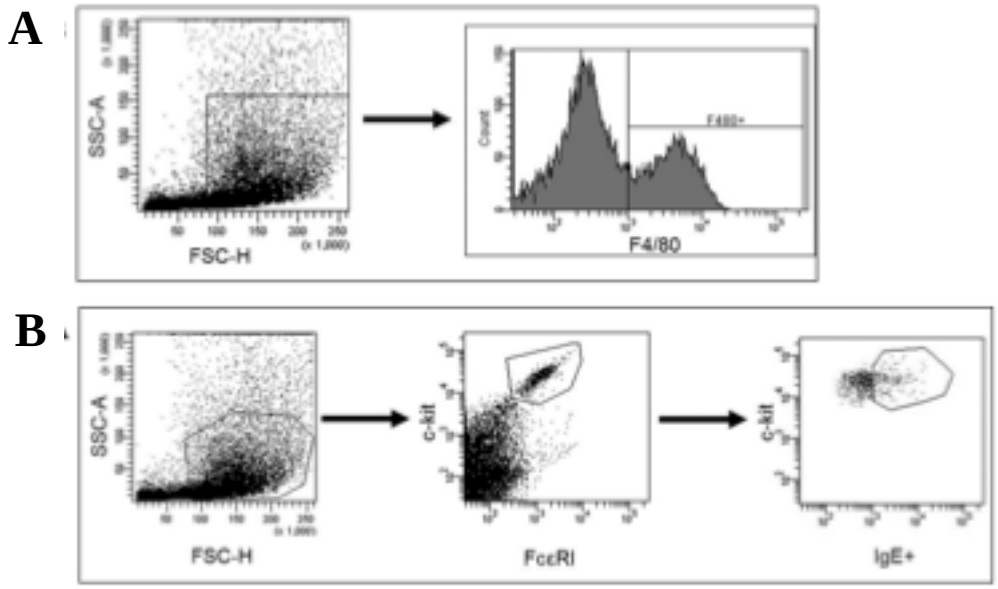

SUPPLEMENTARY FIGURE 4

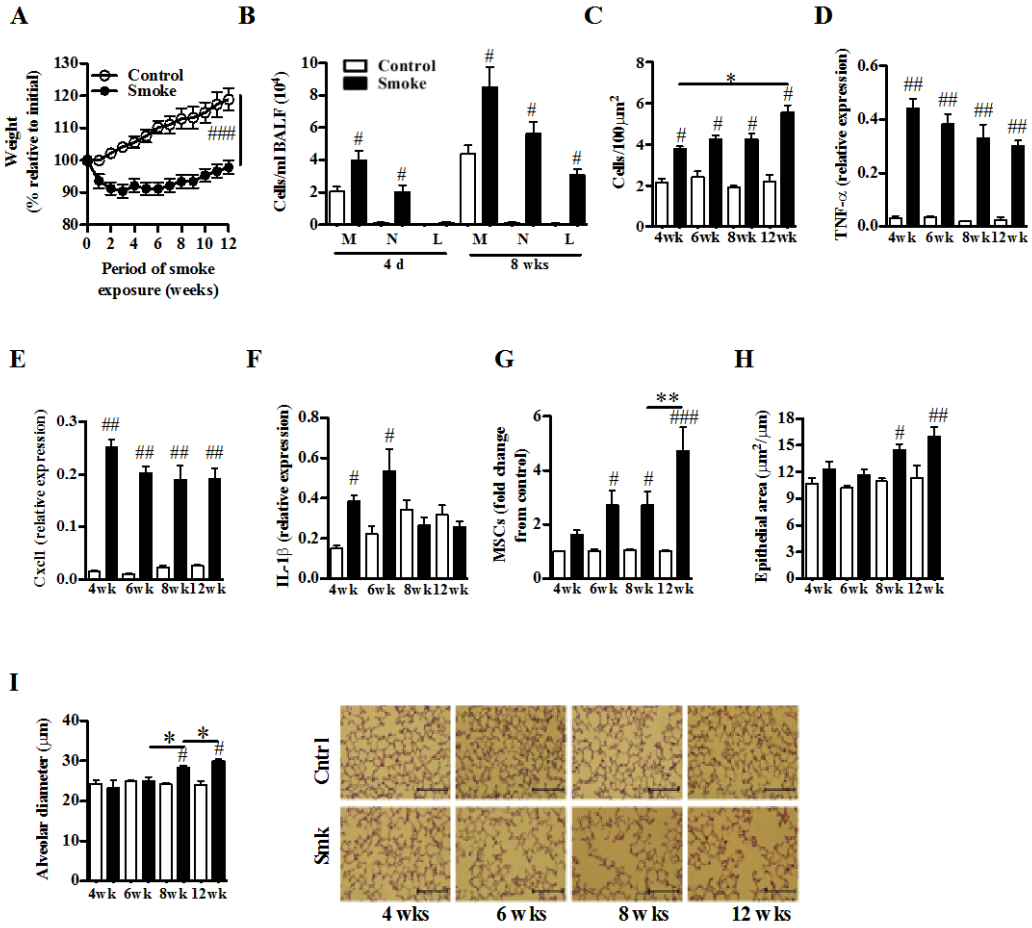
A
B
C
D
Weight (% relative to initial)
Control
Smoke
###
Period of smoke exposure (weeks)
Cells/ml BALF (10^4)
M N L M N L
4 d
8 wks
Cells/100μm^2
4wk 6wk 8wk 12wk
TNF-α (relative expression)
E
F
G
H
Cxcl1 (relative expression)
IL-1β (relative expression)
MSCs (fold change from control)
Epithelial area ($\mu m^2/\mu m$)
I
Alveolar diameter (μm)
Cntrl
Smk
4 wks
6 wks
8 wks
12 wks

FIGURE 1

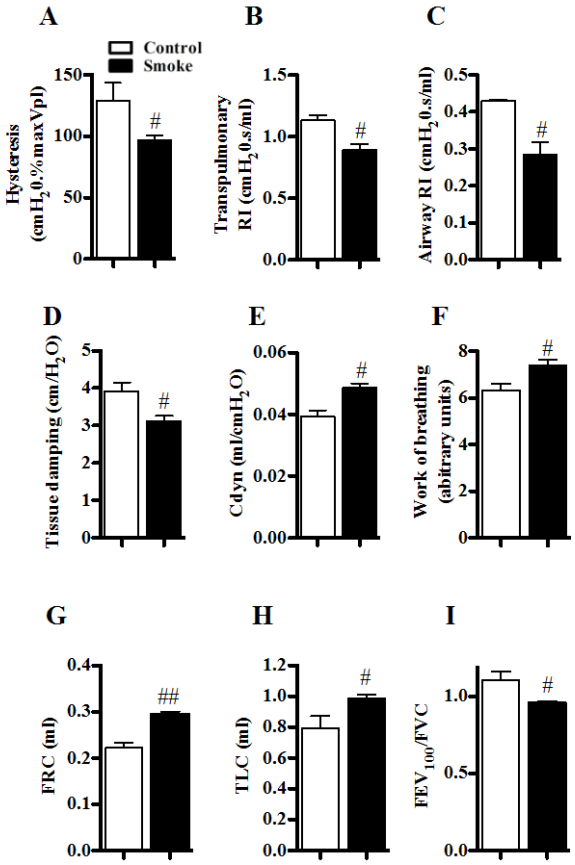
A
B
C
Control
Smoke
Hysteresis (cmH2O.%maxVpl)
Transpulmonary RI (cmH2O.s/ml)
Airway RI (cmH2O.s/ml)
D
E
F
Tissue damping (cm/H2O)
Cdyn (ml/cmH2O)
Work of breathing (abitrary units)
G
H
I
FRC (ml)
TLC (ml)
FEV100/FVC
#
##

FIGURE 2

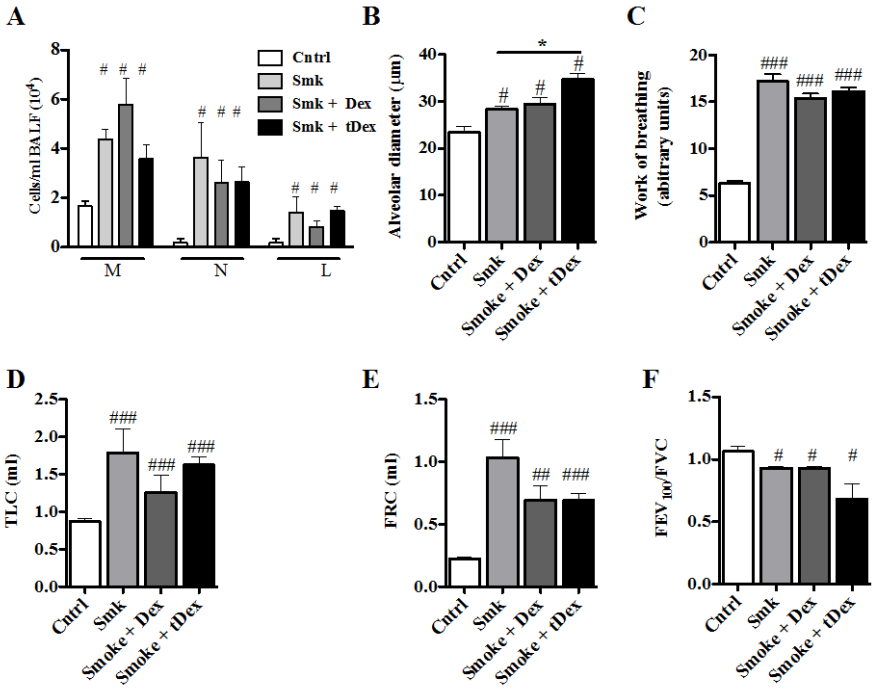
A
B
C
D
E
F
Cells/ml BALF (10⁴)
Cntrl
Smk
Smk + Dex
Smk + tDex
M
N
L
Alveolar diameter (µm)
Work of breathing (abitrary units)
TLC (ml)
FRC (ml)
FEV100/FVC
Cntrl
Smk
Smoke + Dex
Smoke + tDex

Figure 3

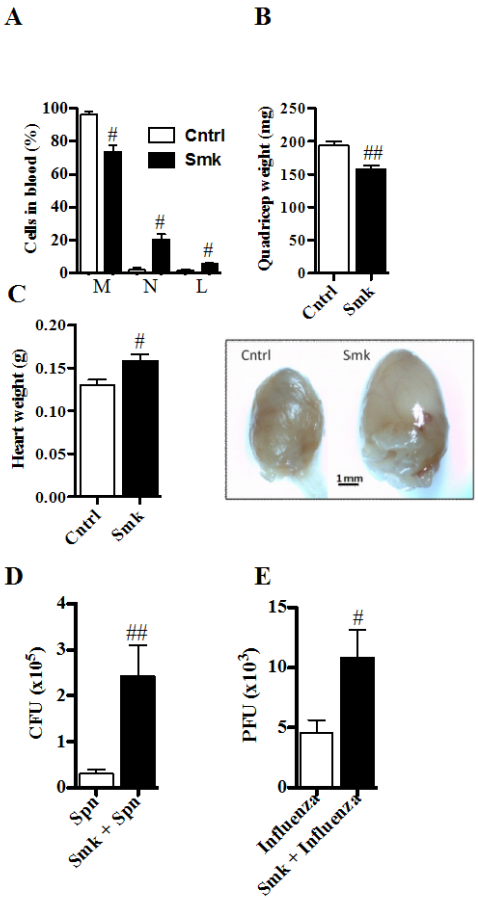
A
B
Cells in blood (%)
Cntrl
Smk
M
N
L
Quadriceps weight (mg)
Cntrl
Smk
C
Heart weight (g)
Cntrl
Smk
Cntrl
Smk
1 mm
D
CFU (x10^5)
Spn
Smk + Spn
E
PFU (x10^3)
Influenza
Smk + Influenza

FIGURE 4

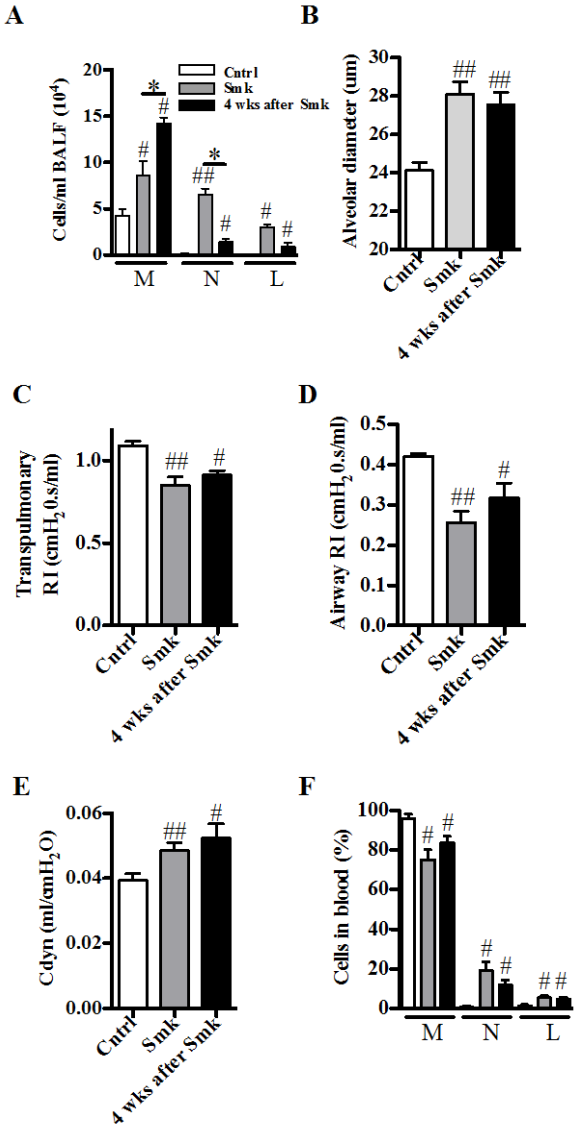
A
B
Cells/ml BALF (10^4)
Cntrl
Smk
4 wks after Smk
M
N
L
Alveolar diameter (um)
C
D
Transpulmonary RI ($cmH_2O.s/ml$)
Airway RI ($cmH_2O.s/ml$)
E
F
Cdyn (ml/cmH_2O)
Cells in blood (%)

Figure 5

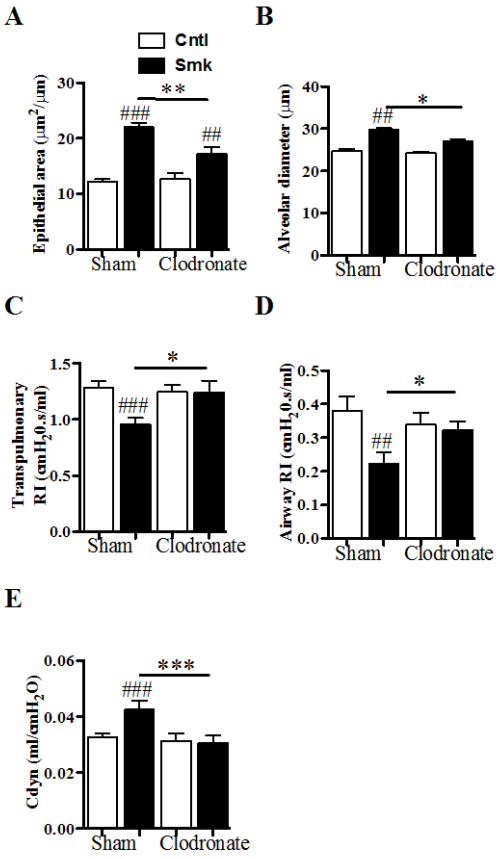
A
B
Cntl
Smk
Epithelial area (μm²/μm)
Alveolar diameter (μm)
Sham
Clodronate
C
D
Transpulmonary RI (cmH2O.s/ml)
Airway RI (cmH2O.s/ml)
E
Cdyn (ml/cmH2O)

FIGURE 6

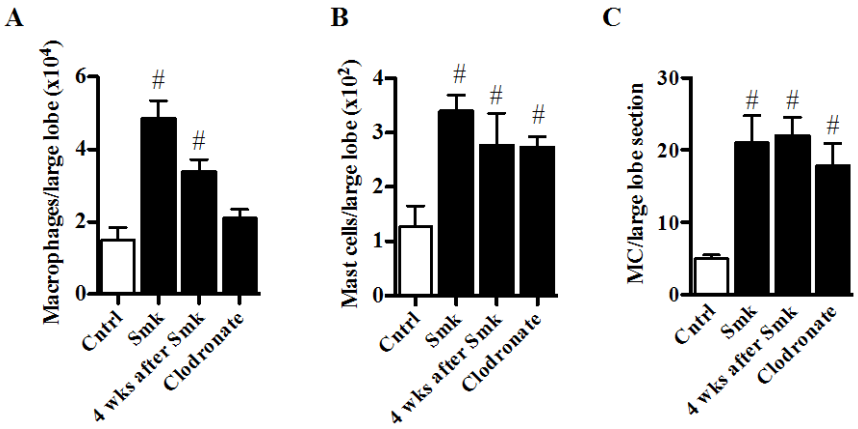
A
B
C
Macrophages/large lobe (x10⁴)
Mast cells/large lobe (x10²)
MC/large lobe section
Cntrl
Smk
4 wks after Smk
Clodronate
#

FIGURE 7

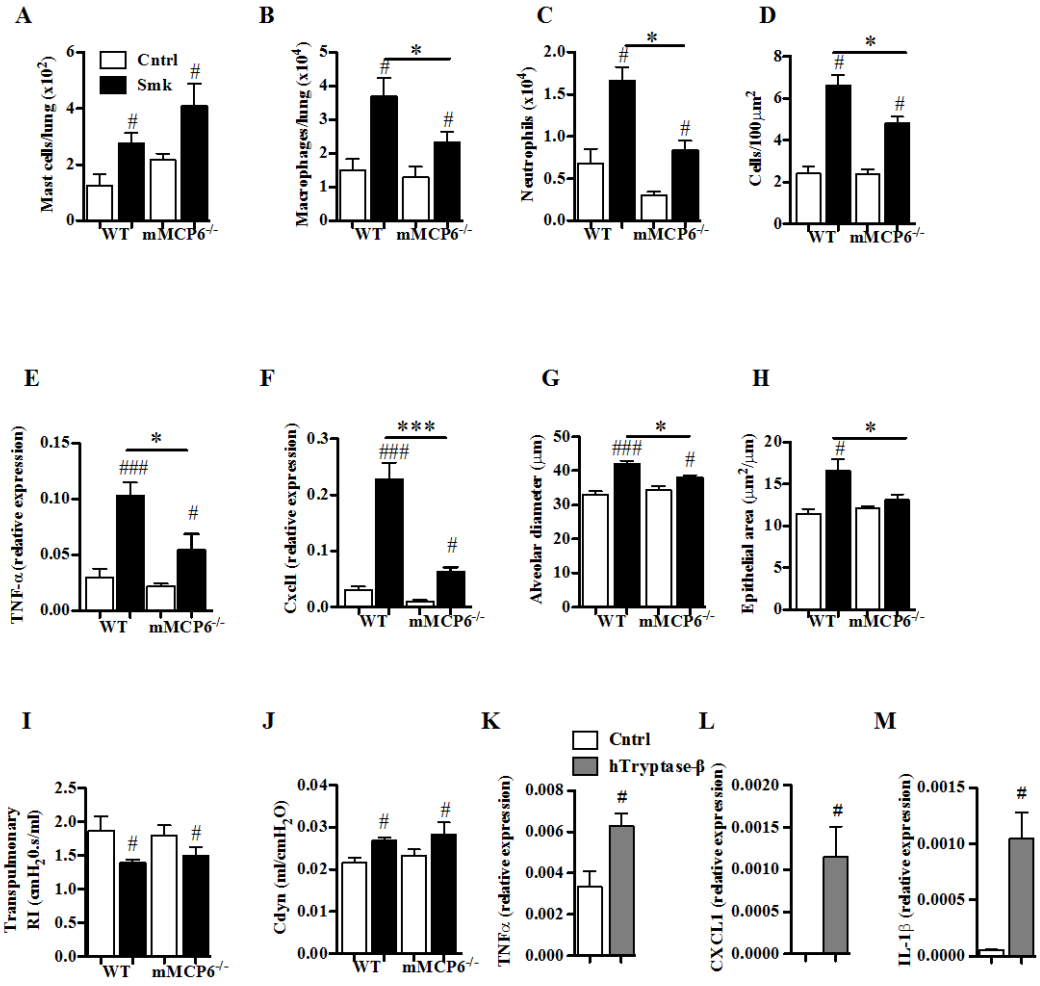
A
B
C
D
Cntrl
Smk
Mast cells/lung (x10²)
Macrophages/lung (x10⁴)
Neutrophils (x10⁴)
Cells/100μm²
WT
mMCP6-/-
E
F
G
H
TNF-α (relative expression)
Cxcl1 (relative expression)
Alveolar diameter (μm)
Epithelial area (μm²/μm)
I
J
K
L
M
Transpulmonary RI (cmH2O.s/ml)
Cdyn (ml/cmH2O)
hTryptase-β
TNFα (relative expression)
CXCL1 (relative expression)
IL-1β (relative expression)

FIGURE 8